Generation of Passive macromodels for lossy multiconductor transmission lines

Original
Generation of Passive macromodels for lossy multiconductor transmission lines / Chinea, Alessandro; GRIVET TALOCIA, Stefano. - STAMPA. - (2007), pp. 61-64. (Intervento presentato al convegno 18th International Zurich Symposium on Electromagnetic Compatibility tenutosi a Munich (Germany) nel 24-28 Sept. 2007) [10.1109/EMCZUR.2007.4388196].

Availability:
This version is available at: 11583/1662808 since: 2015-07-14T09:43:54Z

Publisher:
IEEE

Published
DOI:10.1109/EMCZUR.2007.4388196

Generation of Passive Macromodels for Lossy Multiconductor Transmission Lines

Alessandro Chinea [1], Stefano Grivet-Talocia [2]

Dipartimento di Elettronica, Politecnico di Torino
Corso Duca degli Abruzzi 24, 10129, Torino, Italy
[1]alessandro.chinea@polito.it
[2]stefano.grivet@polito.it

***Abstract*— This paper presents an algorithm for the enforcement of passivity in delay-based multiconductor transmission line macromodels based on the Generalized Method of Characteristics. The algorithm enforces passivity via an iterative procedure based on first-order perturbations. More precisely, the short-circuit admittance matrix of the macromodel is iteratively modified until it becomes positive real. This iterative perturbation is performed on the solutions of a nonlinear eigenvalue problem, whereas the passivity verification is performed using an adaptive frequency sampling process. The proposed technique results in passive, accurate, and efficient macromodels for arbitrary lossy multiconductor transmission lines, which can be synthesized in SPICE netlists for system-level analysis and design.**

I. Introduction

The automated design of highly interconnected systems under Signal Integrity (SI) and Electromagnetic Compatibility (EMC) constraints requires accurate and efficient models for all components. In particular, coupled multiconductor transmission lines still represent a quite challenging modeling task. In fact, all spurious effects that have an influence on the signals must be considered in the models. Most of these effects (e.g., proximity, skin effect losses, dispersion) are natively described in the frequency domain, leading to frequency-dependent per-unit-length parameter matrices. The conversion from frequency to time domain descriptions for transient analysis using standard circuit solvers such as SPICE has been a subject of intense research over the last few decades. Nonetheless, several open problems remain.

This paper deals with one of these problems. Namely, the preservation of passivity during the derivation of a SPICE-compatible transmission line model. This is a fundamental physical property, requiring that no energy can be generated from any passive structure. However, this property may be lost during the model manipulation and approximation steps required for the conversion. It is well-known that non-passive models are unreliable, since they may lead to exponential instability in a transient simulation, depending on their terminations. We concentrate here on models based on the so-called Method of Characteristics (MoC), since it has been demonstrated that such models are the most efficient for lines characterized by a significant propagation delay. Preservation of passivity for such models is still an open issue.

Significant advancements have been recently achieved in [1], [2]. In these papers, the Authors present a systematic procedure for checking the passivity of MoC-based transmission line models. Here, we start from their formulation and we present a perturbation approach that is able to enforce model passivity once some passivity violations have been detected. The results in this work generalize to the multiconductor case the preliminary results in [3], which are valid for single lines only. The basics of MoC formulation are first reviewed in Sec. II, and the passivity check of [1], [2] is outlined in Sec. III in order to set the notations. Also, this section proposes a more robust passivity verification algorithm based on adaptive frequency sampling. Finally, the proposed perturbation scheme is presented in Sec. IV together with two application examples.

II. MoC Macromodels

We consider a multiconductor transmission line of length $\mathcal{L}$ governed by the telegrapher equations, here stated in the Laplace-domain

$$\begin{aligned} -\frac{\mathrm{d}}{\mathrm{d}z}\boldsymbol{V}(z,s) &= \boldsymbol{Z}(s)\boldsymbol{I}(z,s) \\ -\frac{\mathrm{d}}{\mathrm{d}z}\boldsymbol{I}(z,s) &= \boldsymbol{Y}(s)\boldsymbol{V}(z,s) \end{aligned} \tag{1}$$

where z represents the longitudinal coordinate along which signals propagate. The matrices $\boldsymbol{Z}(s)$ and $\boldsymbol{Y}(s)$ denote the f-PUL (frequency dependent per-unit-length) impedance and admittance parameters, respectively. Following the Method of Characteristics (MoC) approach, the solution of telegrapher equations is obtained as [4]

$$\begin{aligned} \boldsymbol{I}_1(s) &= \boldsymbol{Y}_c(s)\boldsymbol{V}_1(s) - \boldsymbol{Q}(s)[\boldsymbol{Y}_c(s)\boldsymbol{V}_2(s) + \boldsymbol{I}_2(s)] \\ \boldsymbol{I}_2(s) &= \boldsymbol{Y}_c(s)\boldsymbol{V}_2(s) - \boldsymbol{Q}(s)[\boldsymbol{Y}_c(s)\boldsymbol{V}_1(s) + \boldsymbol{I}_1(s)] \end{aligned} \tag{2}$$

where $\boldsymbol{V}_{1,2}(s)$ and $\boldsymbol{I}_{1,2}(s)$ represent the terminal voltages and currents of the line and where $\boldsymbol{Q}(s) = \exp\{-\boldsymbol{\Gamma}(s)\mathcal{L}\}$, $\boldsymbol{\Gamma}^2(s) = \boldsymbol{Y}(s)\boldsymbol{Z}(s)$, and $\boldsymbol{Y}_c(s) = \boldsymbol{\Gamma}^{-1}(s)\boldsymbol{Y}(s)$. A SPICE-compatible stamp is derived from (2) by extracting the asymptotic modal delays $\boldsymbol{T} = \mathrm{diag}\{T_k\}$ from the propagation operator $\boldsymbol{Q}(s)$

$$\boldsymbol{P}(s) = e^{-s\boldsymbol{T}}\boldsymbol{M}^{-1}\boldsymbol{Q}(s)\boldsymbol{M} \tag{3}$$

using the asymptotic modal decomposition matrix $\boldsymbol{M}$, and by approximating the remaining matrix operators $\boldsymbol{Y}_c(s)$, $\boldsymbol{P}(s)$ with low-order rational functions $\tilde{\boldsymbol{Y}}_c(s)$, $\tilde{\boldsymbol{P}}(s)$, respectively.

The well-known Vector Fitting algorithm [5] can be used for this task, leading to a state-space realization for $\tilde{\boldsymbol{Y}}_c(s)$

$$\tilde{\boldsymbol{Y}}_c(s) = \boldsymbol{C}(s\boldsymbol{I} - \boldsymbol{A})^{-1}\boldsymbol{B} + \boldsymbol{D}\,, \tag{4}$$

and similarly for $\tilde{\boldsymbol{P}}(s)$. Note that the model poles are the eigenvalues of $\boldsymbol{A}$, whereas the corresponding residues are stored in matrix $\boldsymbol{C}$. The passivity of (4) can be enforced using known techniques [7]. We remark that the macromodel (2)-(4) can be directly synthesized in a compact SPICE subcircuit including ideal delay elements and lumped resistors, capacitors, and controlled sources [4].

III. Passivity characterization

Following [1], [2], the passivity of the line MoC macromodel is here characterized using the short-circuit admittance matrix $\mathcal{Y}(s)$. The latter is readily obtained from (2)–(3) and reads

$$\mathcal{Y}(s) = \begin{bmatrix} \boldsymbol{W}_0^{-1}(s)\boldsymbol{W}_1(s)\tilde{\boldsymbol{Y}}_c(s) & \boldsymbol{W}_0^{-1}(s)\boldsymbol{W}_2(s)\tilde{\boldsymbol{Y}}_c(s) \\ \boldsymbol{W}_0^{-1}(s)\boldsymbol{W}_2(s)\tilde{\boldsymbol{Y}}_c(s) & \boldsymbol{W}_0^{-1}(s)\boldsymbol{W}_1(s)\tilde{\boldsymbol{Y}}_c(s) \end{bmatrix} \tag{5}$$

where

$$\begin{aligned} \boldsymbol{W}_0 &= \boldsymbol{I} - \boldsymbol{M}\mathrm{e}^{-s\boldsymbol{T}}\tilde{\boldsymbol{P}}(s)\mathrm{e}^{-s\boldsymbol{T}}\tilde{\boldsymbol{P}}(s)\boldsymbol{M}^{-1} \\ \boldsymbol{W}_1 &= \boldsymbol{I} + \boldsymbol{M}\mathrm{e}^{-s\boldsymbol{T}}\tilde{\boldsymbol{P}}(s)\mathrm{e}^{-s\boldsymbol{T}}\tilde{\boldsymbol{P}}(s)\boldsymbol{M}^{-1} \\ \boldsymbol{W}_2 &= -2\boldsymbol{M}\mathrm{e}^{-s\boldsymbol{T}}\tilde{\boldsymbol{P}}(s)\boldsymbol{M}^{-1}\,, \end{aligned} \tag{6}$$

with $\boldsymbol{I}$ denoting the identity matrix. A multiport described by the admittance matrix $\mathcal{Y}(s)$ is passive if and only if $\mathcal{Y}(s)$ is positive real [6]. If $\tilde{Y}_c(s)$, $\tilde{P}(s)$, and $\mathcal{Y}(s)$ are asymptotically stable (do not have poles in the right-half plane of the s-domain) with $\tilde{P}(s) \to 0$ for $s \to \infty$, the positive realness of $\mathcal{Y}(s)$ is equivalent to the condition

$$2\mathcal{G}(s) = \mathcal{Y}^T(-s) + \mathcal{Y}(s) \geq 0\,, \quad \forall s = j\omega\,, \tag{7}$$

which can be verified by checking that all eigenvalues $\lambda_\nu(j\omega)$ of $\mathcal{G}(j\omega)$ are nonnegative throughout the frequency axis,

$$\lambda_\nu(j\omega) \geq 0\,, \quad \forall\omega\,. \tag{8}$$

At least two options are available for checking (8). A direct check at discrete frequencies is straightforward but may lead to miss passivity violations in case the sampling is not accurate enough. A second purely algebraic technique, which does not require any frequency sampling, was presented in [1], [2]. This formulation involves restating the macromodel in time-domain as a set of Algebraic Delay-Differential Equations (ADDE), for which a delayed state-space realization is readily obtained from (8) using inverse Laplace transform (see [1], [2] for details). Then, the passivity of the MoC macromodel is guaranteed when there are no purely imaginary values for s that satisfy the following Frequency-Dependent Eigenvalue Problem (FD-EP)

$$s\boldsymbol{\xi} = \boldsymbol{H}(s)\boldsymbol{\xi}\,, \tag{9}$$

where

$$\boldsymbol{H}(s) = \boldsymbol{\mathcal{V}} + \boldsymbol{\mathcal{W}}^- e^{-sT} + \boldsymbol{\mathcal{W}}^+ e^{sT}\,. \tag{10}$$

The constant matrices $\boldsymbol{\mathcal{V}}$ and $\boldsymbol{\mathcal{W}}^\pm$ are easily constructed following a tedious but simple algebraic manipulation, using as building blocks the state-space matrices defining the ADDEs above. We remark that, as a result, matrix $\boldsymbol{H}(s)$ is a quadratic function of the state-space matrix $\boldsymbol{C}$ of (4) for any fixed frequency s. Note that the frequency-dependent matrix $\boldsymbol{H}(s)$ provides a generalization of the concept of Hamiltonian matrices [7] to the ADDE case. Hence, the purely imaginary eigenvalues of FD-EPs above, if any, correspond to those frequencies at which the eigenvalues of $\mathcal{G}(j\omega)$ change sign (Fig. 1). If no such solutions are found, the eigenvalues remain positive at all frequencies and the model is passive.

The above formulation is very appealing, since a global passivity check is provided by the solution of an eigenvalue problem. Unfortunately, the solution of (9) poses serious numerical challenges. In fact, the standard procedure involves its transformation into a larger-size linear eigenvalue problem which is often characterized by several eigensolutions that are very close one to each other. Due to intrinsic ill-conditioning, a test to ascertain whether these solutions are purely imaginary is very difficult. For this reason, we use a less elegant but more robust technique for the detection of these solutions, based on an accuracy-controlled adaptive sampling strategy similar to [8].

We begin by extracting an initial set of frequency samples. Then, this set is adaptively refined until all frequencies

$$\omega_k: \quad \lambda_\nu(j\omega_k) = 0 \tag{11}$$

for some ν are found within an arbitrary precision ϵ. This success of this procedure is guaranteed when: *i.)* the initial samples cover the bandwidth where all solutions are expected; and *ii.)* the sampling rate is sufficiently fine to bracket each interval where no more than two solutions are expected. A high frequency bound exists due to the underlying assumption $\tilde{P}(s) \to 0$ for $s \to \infty$, implying that the eigenvalues $\lambda_\nu(j\omega) \to \mu_\nu$ for $\omega \to \infty$, where $2\mu_\nu = \mathrm{eig}\{\boldsymbol{D} + \boldsymbol{D}^T\} \geq 0$ by construction due to the passivity of (4). The initial sampling rate $\delta\omega$ is determined by insuring that $\delta\omega < 2\pi/(NT_{\max})$, where $T_{\max}$ is the largest extracted delay and $N \geq 40$. For additional details on the adaptive refinement scheme see [8].

IV. Passivity enforcement

Once the above procedure for passivity characterization is applied to a given MoC model, and the model is found to be non-passive, some correction must be applied in order to enforce its passivity. Let us consider the example in Fig. 1. In this case, four frequencies ω_k are found, either as solutions of the FD-EP in (9) or from adaptive frequency sampling, leading to two separate frequency bands where passivity violations occur. In the following sections, we describe a procedure that allows to perturb matrix $\boldsymbol{C}$ in (4) (i.e., the residues of a partial fraction expansion of $\tilde{\boldsymbol{Y}}_c$) so that the non-passive bands are eliminated. This is accomplished by a first-order perturbation of the frequencies ω_k. In fact, this is the main contribution of this work, namely an extension of the perturbation scheme of [7], which is applicable to lumped

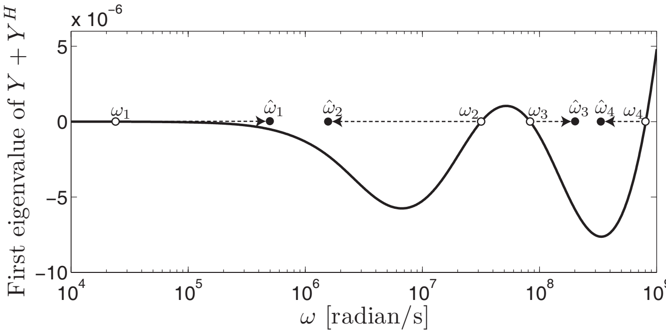

Fig. 1. Modeling a $\mathcal{L} = 10$ cm microstrip ($w = 0.007''$ and $t = 0.0014''$) over a $h = 1/16''$ FR4 substrate with permettivity $\varepsilon_r = 4.7$. Solutions ω_k of the FD-EP and their perturbation $\hat{\omega}_k$. The solid line depicts $\lambda_1(j\omega)$ as in (8)

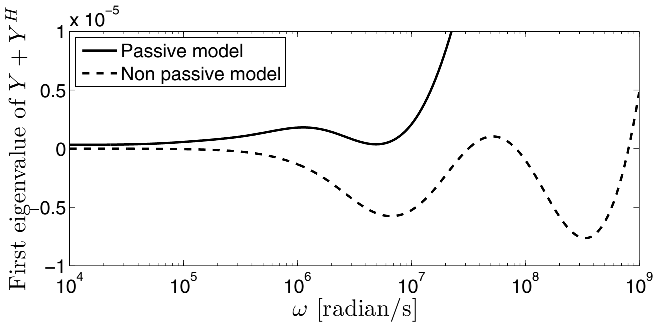

Fig. 2. Eigenvalue $\lambda_1(j\omega)$ of original and perturbed model. The perturbed model is passive because the eigenvalue is positive for all values of ω.

models only, to the delayed transmission-line case. Section IV-A provides a general result on the perturbation of nonlinear eigenvalue problems such as the FD-EP in (9). Section IV-B applies this result for the MoC passivity enforcement.

A. Perturbation of eigenvalues

Let us consider the FD-EP

$$\boldsymbol{H}(s,\varepsilon)\boldsymbol{\xi}(\varepsilon) = s\boldsymbol{\xi}(\varepsilon)\,, \tag{12}$$

where the system matrix depends on an additional parameter $\varepsilon \simeq 0$. We denote a generic eigensolution of (12) as $\{s(\varepsilon), \boldsymbol{\xi}(\varepsilon), \boldsymbol{\zeta}(\varepsilon)\}$, where $\boldsymbol{\xi}$ and $\boldsymbol{\zeta}$ are the right and left eigenvectors associated to the eigenvalue s, in order to highlight its dependence on ε. Also, we denote the reference eigensolution for $\varepsilon = 0$ as

$$\boldsymbol{H}(s_0,0)\boldsymbol{\xi}_0 = s_0\boldsymbol{\xi}_0\,, \quad \boldsymbol{\zeta}_0^H\boldsymbol{H}(s_0,0) = s_0\boldsymbol{\zeta}_0^H\,, \tag{13}$$

where ^{H} denotes the conjugate transpose. Differentiating (12) with respect to ε and setting $\varepsilon = 0$ in the result, we obtain

$$\left(\boldsymbol{I} - \boldsymbol{H}_0^{(s)}\right) s_0'\boldsymbol{\xi}_0 = \boldsymbol{H}_0^{(\varepsilon)}\boldsymbol{\xi}_0 + \left(\boldsymbol{H}(s_0,0) - s_0\boldsymbol{I}\right)\boldsymbol{\xi}_0'\,, \tag{14}$$

where

$$\boldsymbol{H}_0^{(s)} = \left.\frac{\partial \boldsymbol{H}}{\partial s}\right|_{\substack{s=s_0\\ \varepsilon=0}} \qquad \boldsymbol{H}_0^{(\varepsilon)} = \left.\frac{\partial \boldsymbol{H}}{\partial \varepsilon}\right|_{\substack{s=s_0\\ \varepsilon=0}} \tag{15}$$

and where s_0' and $\boldsymbol{\xi}_0'$ are the first-order perturbation coefficients of eigenvalue and eigenvector, respectively. Premultiplying now by the left eigenvector $\boldsymbol{\zeta}_0^H$ and using (13), we have

$$s_0' = \frac{\boldsymbol{\zeta}_0^H\boldsymbol{H}_0^{(\varepsilon)}\boldsymbol{\xi}_0}{\boldsymbol{\zeta}_0^H\left(\boldsymbol{I} - \boldsymbol{H}_0^{(s)}\right)\boldsymbol{\xi}_0}, \tag{16}$$

which establishes a linear relation between the first-order perturbation coefficients of system matrix $\boldsymbol{H}(s,\varepsilon)$ and the corresponding eigenvalue $s(\varepsilon) \simeq s_0 + s_0'\varepsilon$. Of course, in case of a regular frequency-independent eigenvalue problem, we have $\boldsymbol{H}_0^{(s)} = 0$ and standard perturbation results are obtained [9], [7].

B. MoC passivity enforcement

Equation (16) enables the derivation of a passivity enforcement scheme similar to [7]. Each imaginary eigensolution $s_k = j\omega_k$ is displaced to a target location $\hat{s}_k = j\hat{\omega}_k$ inwards into the violation bandwidth (see Fig. 1). This is obtained by computing a new state-space matrix

$$\widehat{\boldsymbol{C}} = \boldsymbol{C} + \boldsymbol{\Delta} \tag{17}$$

such that the first-order perturbation induced in the system matrix $\boldsymbol{H}(s,\boldsymbol{\Delta})$ has the desired perturbed eigensolution. After some straightforward manipulation of (16) we obtain

$$2\Re\left\{\boldsymbol{z}_k^H\boldsymbol{\Delta}\boldsymbol{x}_k\right\} = (\hat{\omega}_k - \omega_k)\Im\left\{\boldsymbol{\zeta}_k^H\left(\boldsymbol{I} - \boldsymbol{H}_k^{(s)}\right)\boldsymbol{\xi}_k\right\}, \tag{18}$$

to be enforced $\forall k$, where the complex vectors $\boldsymbol{z}_k, \boldsymbol{x}_k$ are easily derived using a first-order expansion of $\boldsymbol{H}(s,\boldsymbol{\Delta})$ in terms of $\boldsymbol{\Delta}$. The final (linear) system to be solved for eigenvalue displacement is obtained via the following equivalence

$$2\Re\left\{\boldsymbol{z}_k^H\boldsymbol{\Delta}\boldsymbol{x}_k\right\} = 2\Re\left\{\boldsymbol{x}_k^T \otimes \boldsymbol{z}_k^H\right\}\mathrm{vec}(\boldsymbol{\Delta}) \quad \forall k\,, \tag{19}$$

where $\otimes$ is the Kronecker product [10] and the operator $\mathrm{vec}(\cdot)$ stacks the columns of its matrix argument. Passivity of the MoC model is enforced by iterative solution of (18)-(19).

C. Example

We apply the proposed methodology for the generation of a passive macromodel of the microstrip line of Fig. 1, which was characterized by four imaginary eigenvalues and two frequency bands with passivity violations. The passivity compensation algorithm of Section IV-B was applied in order to eliminate these violations. Figure 1 provides a schematic view of the compensation process, by highlighting the perturbation that is applied in order to displace the imaginary eigenvalues. The final result after only one iteration (CPU time less than one second) of (18) is a passive macromodel, as depicted in Fig. 2, without any imaginary eigenvalues left. As a confirmation that accuracy is preserved during the passivity enforcement, we report in Fig. 3 the transient solution of non-passive and passive models excited by a pulse with 50 Ω terminations. Both curves are undistinguishable. However, changing the termination into a simple RL load drives the non-passive

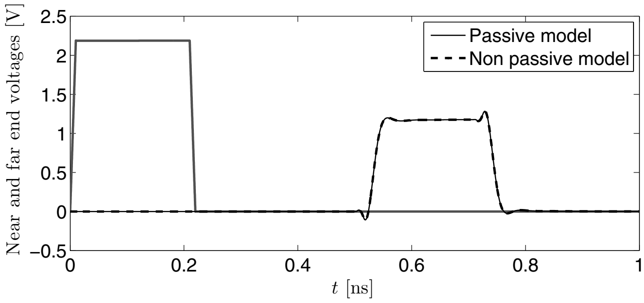

Fig. 3. Comparison of passive and non-passive models with 50 Ω loads.

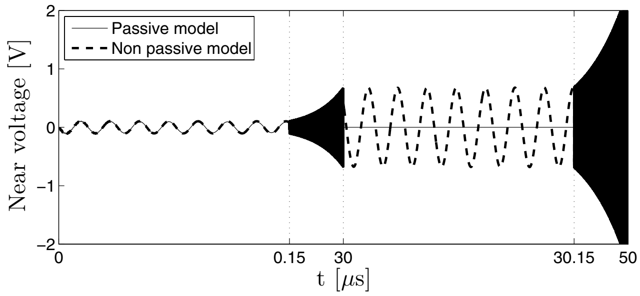

Fig. 4. The non-passive model looses stability when loaded by a simple RL load. A nonuniform scale for the time axis is used to highlight the instability.

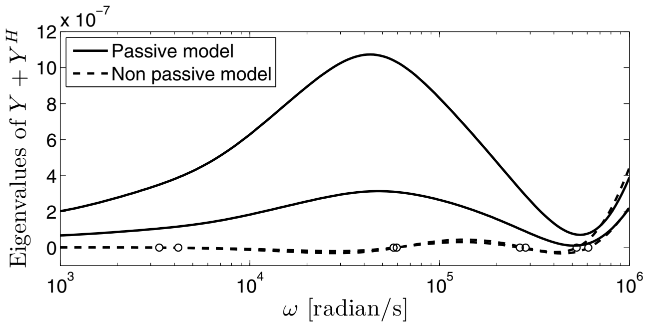

Fig. 5. Eigenvalues $\lambda_\nu(j\omega)$ of original and perturbed passive model of a coupled stripline.

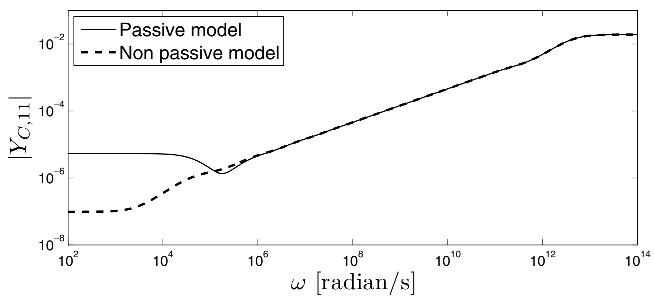

Fig. 6. Characteristic admittance of original and perturbed (passive) model of a coupled stripline.

model to instability, while the passive models remains wel-behaved, see Fig. 4.

We turn now to a multiconductor line, by considering a 3 cm coupled stripline (conductor width and separation $w = s = 6$ mils, thickness $t = 17.5\,\mu$m, total dielectric height $h = 20$ mils, $\varepsilon_r = 4.7$). A MoC macromodel was generated and tested for passivity using the technique of Sec. III. The results are depicted in Fig. 5, showing that there are four passivity violation intervals, two for each eigenvalue λ_ν with $\nu = 1, 2$. The other two eigenvalues $\lambda_{3,4}$ (not shown) did not present any passivity violations. The proposed passivity enforcement scheme was then applied, achieving global passivity in 2 iterations (CPU time about 10 seconds) . The results of the compensation are depicted in Fig. 5, where the two eigenvalues of the passive model are compared to the original eigenvalues. Figure 6 shows a comparison between original and passive models for one element of the characteristic admittance matrix. Small differences are mostly localized where original passivity violations were detected, whereas a good match is preserved elsewhere.

V. Conclusions

We have presented a new algorithm for the passivity enforcement in lossy multiconductor transmission-line macromodels based on the generalized Method of Characteristic. The proposed technique is able to perturb the model coefficients until passivity is achieved. The main algorithm extends to delay-extraction based macromodels existing methodologies that were available only for lumped macromodels. The final outcome is a passive equivalent circuit of the transmission line. This circuit can be used for standard frequency-domain analysis, e.g. based on commonly adopted scattering formalism. In addition, the explicit passivity enforcement allows its safe use in transient analyses including nonlinear terminations, since stability problems are excluded by construction.

References

[1] E. Gad, C. Chen, M. Nakhla, R. Achar, “A Passivity Checking Algorithm for Delay-Based Macromodels of Lossy Transmission Lines,” in *9th IEEE Workshop on Signal Propagation on Interconnects*, 10-13 May 2005, pp. 125–128.

[2] E. Gad, C. Chen, M. Nakhla, R. Achar, “Passivity Verification in Delay-Based Macromodels of Electrical Interconnects,” *IEEE Trans. CAS-I*, Vol. 52, No. 10, Oct. 2005, pp. 2173–2187.

[3] A. Chinea, S. Grivet-Talocia, “A Passivity Enforcement Scheme for Delay-Based Transmission Line Macromodels”, *IEEE Microwave and Wireless Components Letters*, 2007, in press.

[4] S. Grivet-Talocia, H. M. Huang, A. E. Ruehli, F. Canavero, I. M. Elfadel, ”Transient Analysis of Lossy Transmission Lines: an Effective Approach Based on the Method of Characteristics” , *IEEE Trans. Advanced Packaging*, pp. 45–56, vol. 27, n. 1, Feb. 2004.

[5] B. Gustavsen, A. Semlyen, “Rational approximation of frequency responses by vector fitting”, *IEEE Trans. Power Delivery*, Vol. 14, July 1999, pp. 1052–1061.

[6] E. S. Kuh and R. A. Rohrer, *Theory of Linear Active Networks*. San Francisco, CA: Holden-Day, 1967.

[7] S. Grivet-Talocia, “Passivity enforcement via perturbation of Hamiltonian matrices”, *IEEE Trans. CAS-I*, pp. 1755-1769, vol. 51, n. 9, 2004

[8] S. Grivet-Talocia, “Improving the efficiency of passivity compensation schemes via adaptive sampling”, *14th IEEE Topical Meeting on Electrical Performance of Electronic Packaging*, Austin, Texas (USA), October 24–26, 2005, pp. 231–234.

[9] J. H. Wilkinson, *The algebraic eigenvalue problem*, Oxford University Press, London, 1965.

[10] J. W.Brewer, “Kronecker Products and Matrix Calculus in System Theory,” *IEEE Trans. CAS*, Vol. 25, No. 9, Sept. 1978, pp. 772–781.